PPARα-targeted mitochondrial bioenergetics mediate repair of intestinal barriers at the host–microbe intersection during SIV infection

Katti R. Crakes[a], Clarissa Santos Rocha[a], Irina Grishina[a], Lauren A. Hirao[a], Eleonora Napoli[b], Christopher A. Gaulke[a,1], Anne Fenton[a], Sandipan Datta[b], Juan Arredondo[a], Maria L. Marco[c], Sumathi Sankaran-Walters[a], Gino Cortopassi[b], Cecilia Giulivi[b,d], and Satya Dandekar[a,2]

[a]Department of Medical Microbiology & Immunology, University of California Davis School of Medicine, Davis, CA 95616; [b]Department of Molecular Biosciences, School of Veterinary Medicine, University of California, Davis, CA 95616; [c]Department of Food Science & Technology, University of California, Davis, CA 95616; and [d]Medical Investigations of Neurodevelopmental Disorders Institute, University of California, Davis, CA 95616

Chronic gut inflammatory diseases are associated with disruption of intestinal epithelial barriers and impaired mucosal immunity. HIV-1 (HIV) causes depletion of mucosal CD4$^+$ T cells early in infection and disruption of gut epithelium, resulting in chronic inflammation and immunodeficiency. Although antiretroviral therapy (ART) is effective in suppressing viral replication, it is incapable of restoring the "leaky gut," which poses an impediment for HIV cure efforts. Strategies are needed for rapid repair of the epithelium to protect intestinal microenvironments and immunity in inflamed gut. Using an in vivo nonhuman primate intestinal loop model of HIV/AIDS, we identified the pathogenic mechanism underlying sustained disruption of gut epithelium and explored rapid repair of gut epithelium at the intersection of microbial metabolism. Molecular, immunological, and metabolomic analyses revealed marked loss of peroxisomal proliferator-activated receptor-α (PPARα) signaling, predominant impairment of mitochondrial function, and epithelial disruption both in vivo and in vitro. To elucidate pathways regulating intestinal epithelial integrity, we introduced probiotic *Lactobacillus plantarum* into Simian immunodeficiency virus (SIV)-inflamed intestinal lumen. Rapid recovery of the epithelium occurred within 5 h of *L. plantarum* administration, independent of mucosal CD4$^+$ T cell recovery, and in the absence of ART. This intestinal barrier repair was driven by *L. plantarum*-induced PPARα activation and restoration of mitochondrial structure and fatty acid β-oxidation. Our data highlight the critical role of PPARα at the intersection between microbial metabolism and epithelial repair in virally inflamed gut and as a potential mitochondrial target for restoring gut barriers in other infectious or gut inflammatory diseases.

HIV/AIDS | SIV | gut epithelium | mitochondria | PPARα

Current antiretroviral therapy (ART) has transformed HIV-1 (HIV) infection into a manageable chronic disease, but not consistently led to complete immune recovery (1). Gut-associated lymphoid tissue is an early target of HIV for establishment of persistent viral reservoirs and chronic inflammation. Severe loss of mucosal CD4$^+$ T cells and disruption of gut epithelial barriers occur very early in HIV infection in humans and in Simian immunodeficiency virus (SIV)-infected nonhuman primate model of AIDS, and precede CD4$^+$ T cell loss in peripheral blood (2, 3). Importantly, early onset of gut epithelial barrier disruption occurs prior to severe mucosal CD4$^+$ T cell depletion and was attributed to mucosal IL-1β production and NF-κB activation (4). Initiation of ART during early HIV and SIV infections lead to recovery of mucosal CD4$^+$ T cells and gut epithelial barriers, while the recovery is substantially delayed or incomplete when ART is initiated late during infection (5–8). Leaky gut epithelial barriers and loss of Th17 CD4$^+$ T cell responses contribute to microbial translocation and to mucosal and systemic inflammation (9–11). Although ART is effective in suppressing HIV production, it does not have capacity to target the repair of dis-

rupted gut mucosal compartment. Therapeutic interventions that also target epithelial barrier repair for HIV infection need further investigation.

Mitochondria are the main source of energy metabolism and serve as master regulators for the cell survival, function, metabolism, and immunity (12). Mitochondrial dysfunction, manifested as increased mitochondrial free-radical production and reduced ATP production, is reported in acute and chronic gastrointestinal diseases with impaired epithelial barriers (13). However, a critical gap of knowledge exists at understanding the role of mitochondrial metabolism and function in the gut epithelial barrier integrity in HIV and SIV infections. Mitochondrial dysfunction exhibited by altered oxidative phosphorylation and fatty acid oxidation was observed in CD4$^+$ T cells from HIV$^+$ immunologic

Significance

Our study has identified that impaired peroxisome proliferator-activated receptor-α (PPARα) signaling and associated mitochondrial dysfunction is an important underlying mechanism for prolonged leaky gut barriers in HIV and Simian immunodeficiency virus (SIV) infections despite antiretroviral therapy. Using the intestinal loop model in SIV-infected rhesus macaques, we found rapid repair of gut epithelial barriers within 5 h of administering *Lactobacillus plantarum* into virally inflamed gut. The rapid recovery was driven by PPARα activation and occurred independent of mucosal CD4$^+$ T cell recovery, highlighting a metabolic repair pathway that can be targeted for epithelial repair prior to complete immune recovery. Our findings provide translational insights into restoring gut mucosal immunity and function, both of which are essential to enable HIV cure efforts.

MICROBIOLOGY

nonresponders receiving long-term ART (14). ART-associated lipodystrophy also involves mitochondrial toxicity (15, 16). HIV antigens can induce mitochondrial damage and apoptosis in T and neuronal cell lines in vitro (17, 18). Deciphering the role of mitochondrial function in gut epithelial barrier integrity in vivo can provide new therapeutic strategies for restoring mucosal immunity.

Gut epithelial cell homeostasis is regulated by commensal microbes, which dampen gut inflammation and enhance mucosal immunity to pathogens (19). Dysbiosis of gut microbiota is reported in advanced HIV and SIV infections (20–22). Potential beneficial effects of a commercial probiotic supplementation in HIV-infected individuals could not be distinguished from effects of ART (23). We previously reported that introduction of *Lactobacillus plantarum*, a commensal microbe with probiotic activity, into the small intestinal lumen during early SIV infection rapidly restored the gut epithelial barrier integrity by dampening NF-κB activation and inflammatory cytokine expression (4). However, it is not known whether *L. plantarum* can rapidly target the repair of gut epithelial barriers in vivo during advanced chronic SIV infection, especially prior to mucosal CD4$^+$ T cell restoration. In this study, we utilized an SIV model to investigate mechanisms of gut epithelial barrier dysfunction in chronic SIV infection and to decipher molecular pathways that can directly reverse epithelial damage independent of mucosal immune recovery following *L. plantarum* administration. Mitochondrial metabolic dysfunction was prominent as evidenced by decreased mitochondrial fatty acid β-oxidation and disrupted morphology and correlated with increased IL-1β expression and epithelial barrier disruption. Within 5 h of *L. plantarum* administration, intestinal barrier integrity was rapidly restored by activating peroxisome proliferator-activated receptor-α (PPARα), and enhancing mitochondrial morphology and function and reduced IL-1β production. Remarkably, this repair occurred independent of mucosal CD4$^+$ T cell restoration and in the absence of ART. Fenofibrate, a PPARα agonist, reversed HIV antigen-induced alterations in mitochondrial bioenergetics and epithelial barrier

disruption in epithelial cells in vitro. In summary, we identified a mechanism of PPARα-mediated restoration of mitochondrial function by leveraging *L. plantarum* metabolism to renew the gut epithelium and mucosal immunity and counteract HIV and SIV pathogenic effects.

Results

Increased Mucosal IL-1β Expression Coinciding with Impaired Intestinal Epithelial Barriers in Advanced SIV Infection despite Late Initiation of ART. We previously reported the onset of gut epithelial barrier impairment at 2.5 d post-SIV infection. The disruption of ZO-1 and claudin-1 tight junctions occurred prior to the gut mucosal CD4$^+$ T cell loss and correlated with rapid induction of the proinflammatory cytokine IL-1β in intestinal Paneth cells (4). We sought to determine whether mucosal IL-1β expression persists during chronic SIV infection and contributes to sustained epithelial barrier disruption. Productive viral infection was evident by high levels of SIV RNA (Fig. 1*A*) and CD4$^+$ T cell loss in peripheral blood (Fig. 1*B*), as well in the gut tissue (*SI Appendix*, Fig. S1). Immunohistochemical analysis showed decreased expression of ZO-1 tight junction protein and discontinuous, stippled appearance of its distribution compared to SIV$^-$ controls (Fig. 1 *C* and *D*), suggesting that the gut epithelial barrier disruption persists during chronic SIV infection. Similar changes were detected for other tight junction proteins, including e-cadherin and occludin (*SI Appendix*, Fig. S2). Transcriptomic analysis showed the decreased expression of genes regulating gut barrier function, including adherens junctions, gap junctions, tight junctions, and secretory and digestive enzymes. (*SI Appendix*, Fig. S3). Mucosal IL-1β expression remained elevated during chronic viral infection and was primarily localized to the base of intestinal crypts (Fig. 1 *E* and *F*). Increased expression of the genes downstream to IL-1β signaling was also detected in SIV infection (Fig. 1*G*).

Next, we sought to examine whether initiation of ART in chronic SIV infection and suppression of viral loads would lead to the reduction of gut mucosal IL-1β expression and recovery of
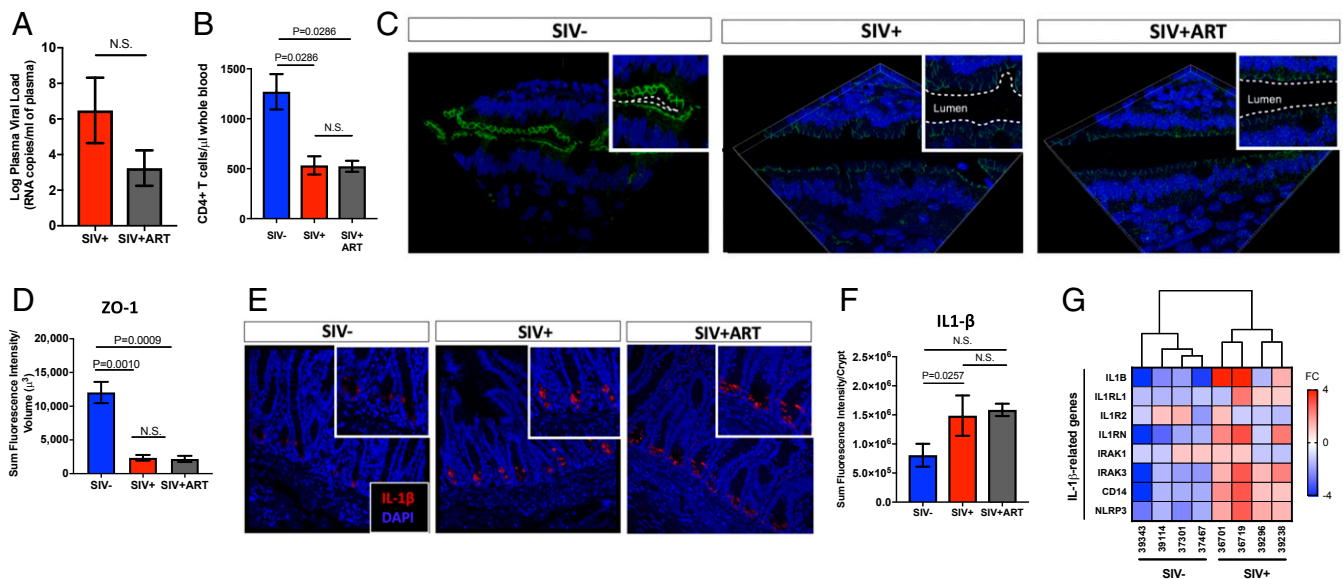
Fig. 1. Gut epithelial barrier disruption, mucosal CD4$^+$ T cell depletion, and IL-1β expression persist in advanced SIV infection despite late initiation of ART. (*A*) Viral loads and (*B*) CD4$^+$ T cell numbers were measured in peripheral blood of SIV-infected rhesus macaques (*n* = 3) and those treated with ART for >10-wk (*n* = 5). (*C*) Immunostaining showed altered distribution of tight junction protein ZO-1 (magnification: 63×) in gut epithelium during SIV infection despite ART, as shown in *D* semiquantitative analysis by Imaris v8.2. (*E*) Production of IL-1β (magnification: 20×) from intestinal crypts was increased in SIV infection and did not change after initiation of ART, as shown by (*F*) semiquantitative analysis on Imaris v8.2. (*G*) A heatmap dendrogram of IL-1β related genes was analyzed from gene-expression microarray of gut tissue. N.S., not significant.

gut epithelium. We obtained gut tissue samples from 8 SIV-infected animals from a previous study (7). ART was initiated at 10-wk postinfection and continued for at least 10 more weeks. ART did not result in complete suppression of plasma viral loads (Fig. 1A) or full CD4$^+$ T cell recovery in both peripheral blood and gut tissue (Fig. 1B and *SI Appendix*, Fig. S1). It did not cause a significant decrease in IL-1β expression in intestinal crypts (Fig. 1 E and F). Thus, the gut mucosal recovery during late ART is not rapid and would require extended therapeutic intervention.

Mitochondrial Impairment and Intestinal Epithelial Barrier Disruption in SIV/HIV Infection. To identify cellular mechanisms contributing to the sustained epithelial barrier dysfunction during chronic SIV infection, we performed an untargeted metabolomic analysis of gut luminal contents from SIV-infected macaques compared to uninfected controls. Detection of metabolites in the luminal compartment revealed new insights on host–microbe interaction, cometabolism, and their common metabolic pathways. These metabolites were produced by gut microbiota and the host. Metabolomic analysis identified pathways of fatty acid metabolism to be highly modulated in SIV infected gut (Fig. 2 A and B, red arrows). An increased accumulation of short- and medium-chain acyl-carnitines compared to free carnitines (Fig. 2C) was observed in SIV infection despite no significant changes in the ratio of long and very-long acylcarnitine to free carnitines (Fig. 2D). This reflected a defect in mitochondrial fatty acid β-oxidation that is independent of carnitine palmitoyl transporters, which shuttle only long-chain fatty acids into the mitochondria (Fig. 2E). If these metabolites are of host origin, our data suggest that impaired mitochondrial fatty acid β-oxidation, which provides significant ATP to gut tissue, may contribute to gut epithelial barrier disruption. As the reducing equivalents from carbohydrates and fatty acids are harnessed by FADH$_2$ and NADH for mitochondrial oxidation at the level of the electron transport chain, the enrichment in tryptophan (Trp) metabolism may suggest an increase in downstream NAD$^+$ metabolism (Fig. 2B). This was supported by higher and lower concentrations of Trp-derived quinolate and nicotinate ribonucleoside, respectively, as a potential mechanism to increase NAD levels via de novo synthesis (*SI Appendix*, Fig. S4A). A reduction in metabolites involved in phospholipid composition was observed in SIV infection, whereas higher trimethylamine N-oxide levels indicate altered cholesterol metabolism with an increased deposition of cholesterol within the gut wall (*SI Appendix*, Fig. S4B). Changes in these processes (i.e., ATP-derived mitochondrial fatty acid oxidation, NAD$^+$ metabolism, and phospholipid contents) may contribute to the decrease in the epithelial barrier integrity. Levels of acylcarnitine metabolites were negatively correlated with tight junction protein ZO-1 expression, highlighting the link between mitochondrial fatty acid β-oxidation and gut permeability in chronic SIV infection in vivo. No significant correlations were found with pyrimidine metabolism (*SI Appendix*, Fig. S5). Transcriptomic analysis revealed reduced mucosal gene expression of proteins associated with fatty acid metabolism in SIV-infected animals compared to uninfected controls, further validating impairment of mitochondrial fatty acid β-oxidation in the gut during SIV infection (Fig. 2F).

The impairment of mitochondrial fatty acid β-oxidation in SIV infection seem to also involve stages of transporting, tagging, and catabolizing fatty acids. Our findings in chronic SIV infection were also found to occur in HIV infection. We analyzed the gene-expression data from our previous study of gut biopsies from therapy-naive patients during primary HIV infection (2). Transcriptomic analyses revealed that the expression of genes involved in fatty acid metabolism was significantly reduced in human gut biopsies during the primary HIV infection (Fig. 2G). The magnitude of this reduction was higher in chronic HIV infection in
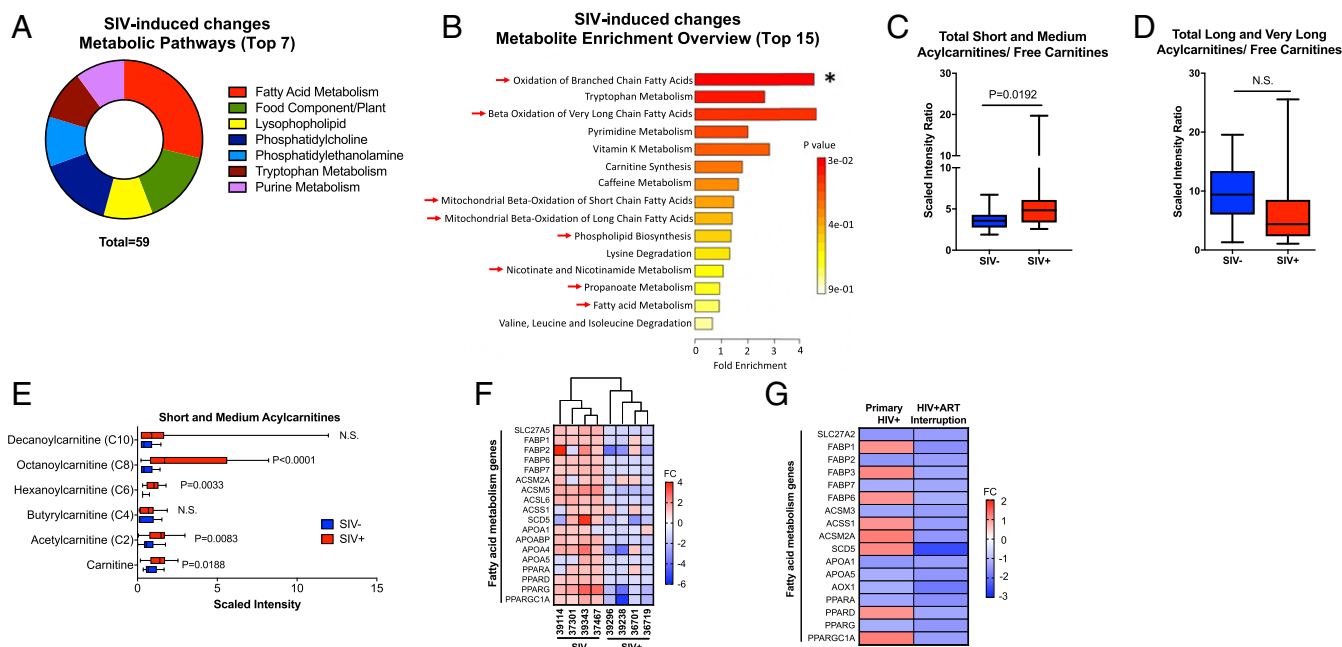
Fig. 2. Gut metabolomic profiling identifies mitochondrial fatty acid β-oxidation as a major target of SIV/HIV infection. (A) Pathway analysis of significantly altered metabolites (q < 0.25, P < 0.05) was performed from ileal luminal contents of SIV-infected macaques compared to healthy controls. (B) Enrichment analysis of significantly up-regulated metabolites (q < 0.25, P < 0.05) was performed using MetaboAnalyst (*P < 0.05). Arrows indicate pathways implicated in metabolic pathways dependent on mitochondrial function. (C) Ratio of short- and medium-chain (C2–10) and (D) long and very-long chain (C12–24) acylcarnitines to free carnitines was measured using UPLC-MS/MS by Metabolon. (E) Significant increases in short- and medium-chain acylcarnitines were detected in chronic SIV infection. (F) Heatmap depicting expression of genes involved in fatty acid metabolism from gut tissue of chronic SIV-infected rhesus macaques (n = 4 in SIV$^-$ group, n = 4 in SIV$^+$ group) and (G) gut biopsies of individuals in primary stage of HIV infection (n = 3 in HIV group, n = 3 in control group) and chronic stage of HIV infection in the absence of ART (n = 4 in HIV group, n = 10 in control group). N.S., not significant.

the absence of ART. While initiation of ART has been shown to exacerbate defects in mitochondrial fatty acid β-oxidation, our data show that these defects are present even in absence of ART in HIV-infected patients, highlighting the direct causal link between SIV/HIV infection and impaired mitochondrial fatty acid metabolism in the gut.

To further define the mechanisms of HIV-induced enteropathy and the direct role of HIV viral proteins (gp120 and Tat) and IL-1β signaling, we assessed gut epithelial cell functionality and permeability using a Caco-2 gut epithelial cell culture model in vitro. Consistent with our findings in HIV and SIV infections in vivo, both IL-1β and the combination of HIV proteins gp120 and Tat induced marked disruption of intestinal barrier integrity and function as detected by decreased expression and distribution of tight junction protein ZO-1 (Fig. 3A) and decreased transepithelial resistance across the cell monolayers (Fig. 3B). This cellular disruption was linked to reduced mitochondrial function as detected by a moderate decrease in mitochondrial ATP-linked oxygen uptake with glucose and glutamine as substrates, demonstrating that mitochondrial dysfunction may underlie epithelial barrier disruption (Fig. 3 C and D). Addition of IL-1β alone to Caco-2 cells reduced the spare respiratory capacity (by less than 25%), suggesting either lower activity of complexes I, III, and IV, or lower mitochondrial mass. However, the combination of HIV gp120 and Tat lowered both basal respiration (by less than 20%) and spare respiratory capacity (by less than 40%) in Caco-2 cells (Fig. 3 E and F). Our findings map the pathogenic effects of HIV antigens to disruption of either complex I, III, IV, or mitochondrial mass. These results are consistent with findings in isolated lymphocytes from HIV-infected patients (24). Our study links mitochondrial impairment to gut epithelial barrier disruption in HIV and SIV infections. To define the precise

role of mitochondrial-derived ATP in regulating epithelial tight junctions, we examined the effect of specific inhibitors of complex I (rotenone), complex III (antimycin), and complex V (oligomycin) individually in inducing disruption of tight junction ZO-1 distribution in Caco-2 cells (Fig. 3G). As expected for mitochondrial poisons that block the mitochondrial ATP production with (antimycin > rotenone > oligomycin) or without significant increased reactive oxygen species (ROS) production (oligomycin), inhibition of complex III or V resulted in marked disruption of ZO-1 distribution, while complex I induced modest changes in ZO-1 expression. These differential effects indicated that increased ROS was not mediating the disruption of ZO-1 expression, that mitochondrial ATP was critical for this expression. These results also underlined the relevance of fatty acid oxidation in which the ratio of $FADH_2$-to-NADH is higher (with lower involvement of complex I) than that of glucose alone. Since these barrier defects were identical to those induced by viral proteins or IL-1β on Caco-2 cells, we hypothesized that mitochondria and catabolism of specific substrates at the mitochondrial level were the target of HIV infection, thereby sustaining gut epithelial disruption.

Rapid Repair of Epithelial Barriers in Chronic SIV Infection Independent of Mucosal CD4+ T Cell Restoration after *L. plantarum* Administration. We sought to explore whether the gut epithelial barrier could be targeted for rapid repair/renewal in HIV infection even during the state of incomplete mucosal immune recovery. We utilized the ligated intestinal loop model in rhesus macaques with chronic SIV infection to examine rapid and direct effects of probiotic *L. plantarum* administration on the recovery of gut epithelial disruption. Intestinal loops in healthy, uninfected controls ($n = 4$) and macaques infected with SIV for 10 wk ($n = 4$) were injected with *L. plantarum* from which tissue samples and luminal contents
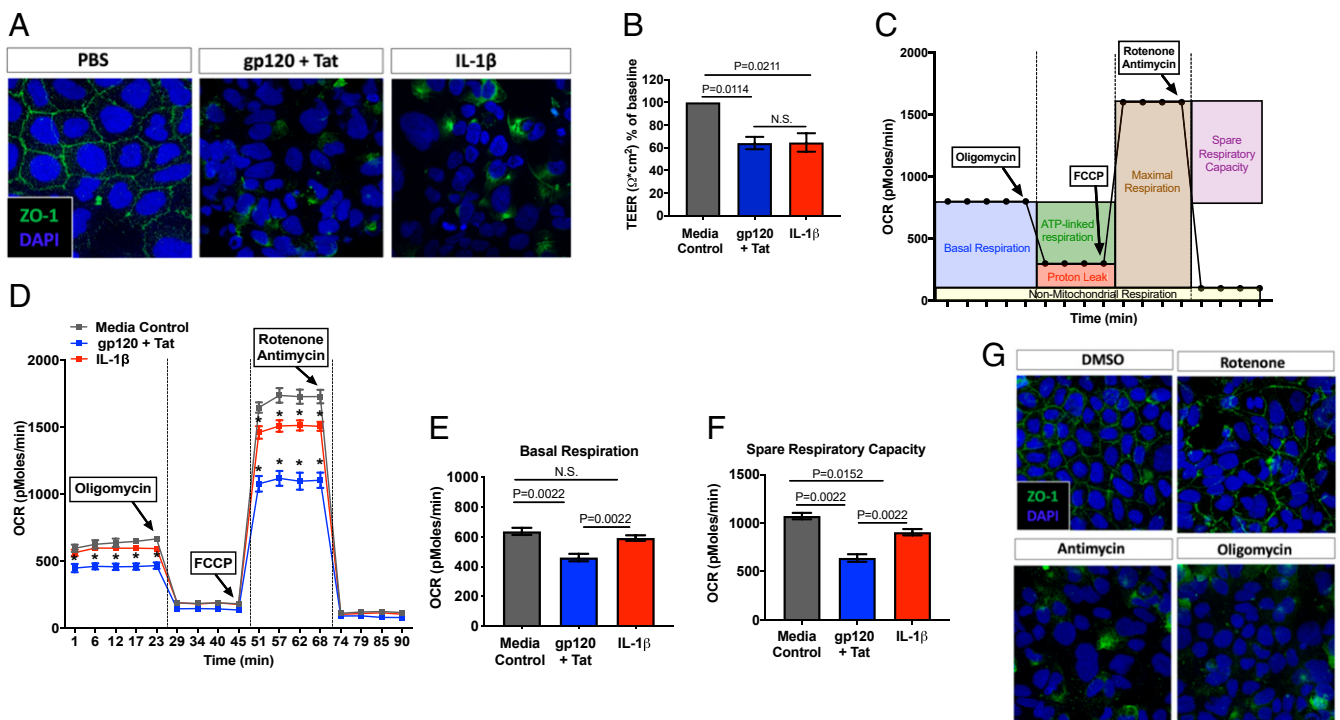
Fig. 3. Gut epithelial tight junctions are disrupted by HIV envelope, Tat, and IL-1β through inhibition of mitochondrial respiration. Epithelial tight junction permeability in Caco-2 cells was measured after 5-h treatment with HIV gp120 (0.1 μg/mL) + Tat (1.4 μg/mL) or IL-1β (10 ng/mL) by (A) distribution of ZO-1 immunostaining (magnification: 63×) and (B) transepithelial electrical resistance (TEER) across the cell monolayer. (C) OCR in Caco-2 cells was detected using Seahorse XFe24 after (D) 5-h treatment with HIV gp120 + Tat or IL-1β, and significant alterations ($P < 0.05$) were observed in (E) basal respiration and (F) spare respiratory capacity. (G) Inhibition of mitochondrial respiration by 5-h treatment with rotenone, antimycin, and oligomycin altered tight junction protein ZO-1 distribution (magnification: 63×) by immunohistochemistry. N.S., not significant.

were analyzed after 5 h (*SI Appendix,* Fig. S6). The 16S rRNA bacterial sequence analysis showed that *L. plantarum* was readily detectable in these loops (*SI Appendix,* Fig. S7*A*) and the viability and metabolic functionality of *L. plantarum* was not impaired in virally infected and inflamed gut or in the context of resident gut microbes (*SI Appendix,* Fig. S7*B*). It was very striking that administration of *L. plantarum* for 5 h significantly increased ZO-1 expression in the epithelium of intestinal loops of chronically SIV-infected animals (Fig. 4*A*), as indicated by quantification of ZO-1 fluorescence intensity (Fig. 4*B*). Transcriptomic analysis revealed a similar trend of increased gene-expression regulating gut barriers following *L. plantarum* administration (Fig. 4*C*). Suppression of WNT pathway genes regulating intestinal homeostasis, proliferation, and differentiation was observed in SIV infection, which was rapidly reversed after *L. plantarum* administration (*SI Appendix,* Fig. S8 *A* and *B*). Increased expression of Ki67, a cell proliferation marker in intestinal crypts was noted (*SI Appendix,* Fig. S8 *C* and *D*). Reduced IL-1β protein production was also seen in intestinal crypts in chronic SIV

infection (Fig. 4 *D* and *E*) and decreased expression of IL-1β and associated genes (Fig. 4*F*) which was verified on qRT-PCR (*SI Appendix,* Fig. S9). No detectable changes were observed in the gut viral loads and laminal propria CD4$^+$ T cell percentages of intestinal loops after administration of *L. plantarum* as compared to untreated controls (*SI Appendix,* Fig. S10). Our results suggest that *L. plantarum* can be used to target intestinal epithelial barrier repair, prior to gut immune cell recovery.

L. plantarum-Induced Intestinal Epithelial Repair In Vivo through Mitochondrial Rescue. We investigated the capacity of *L. plantarum* to repair gut epithelial barrier disruption in SIV infection through rapid rescue of cellular, molecular, and functionality of mitochondria. We examined mitochondrial morphology (by transmission electron microscopy, TEM), mitochondrial gene expression (DNA microarrays), and mitochondrial metabolism (metabolomics) in intestinal tissues and their contents.

Electron micrographs revealed a large number of mitochondria located at the apical end adjacent to epithelial cell junctions
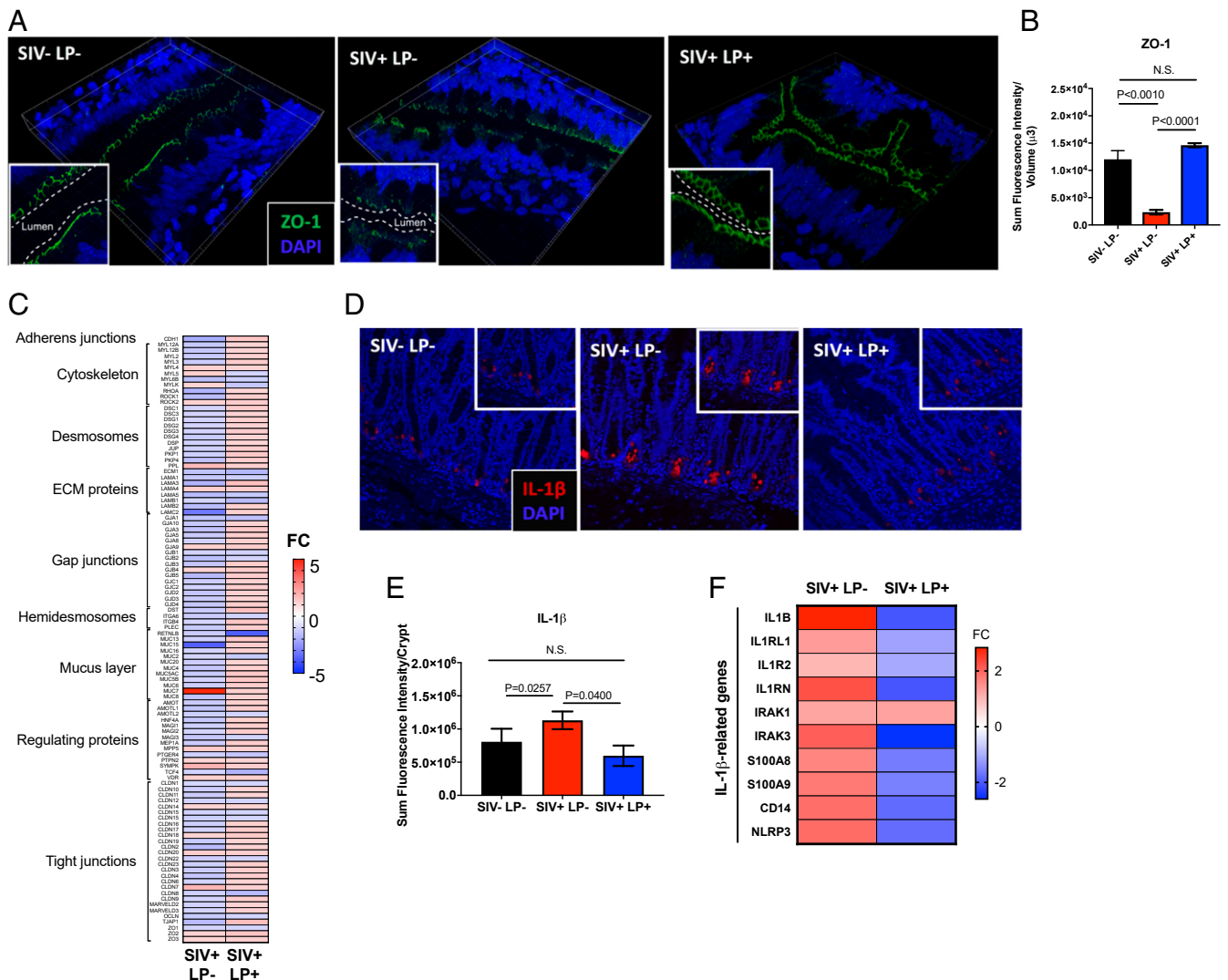
Fig. 4. *L. plantarum* rapidly repairs epithelial barriers in chronic SIV infection in the absence of mucosal CD4$^+$ T cell restoration. Evaluation of epithelial barrier integrity after 5 h of incubation with *L. plantarum* was measured by (*A*) immunohistochemical staining of ZO-1 protein (magnification: 63×), (*B*) semiquantitated using Imaris v8.2, and (*C*) broad transcriptomics analysis of genes involved in gut barrier function. Localization of IL-1β (magnification: 20×) in intestinal crypts was (*D*) detected by immunohistochemical staining and (*E*) semiquantitated using Imaris v8.2. (*F*) Heatmap of genes associated with IL-1β expression was analyzed using gene-expression microarrays of ileal tissues. N.S., not significant.

that provide contact between neighboring cells in the ileum (Fig. 5A). These findings suggest the dominant role of mitochondrial ATP at sustaining the functionality of epithelial tight junctions. Images from the ileum of healthy SIV⁻ animals showed that total mitochondria occupied about 20% of each high-power field (Fig. 5B) with an average mitochondrial area of 0.1 μm² (Fig. 5C). Mitochondrial matrix exhibited parallel stacks of ordered cristae with light intracrystal space and dark matrix. Intracellular mitochondrial distribution seemed mostly aligned longitudinally, parallel, and in close proximity to tight junctions. In SIV-infected tissues, mitochondrial mass was decreased by almost half, with a more circular and less tubular shape characteristic of damage mitochondria undergoing fission, a process that is typically followed by autophagy or mitophagy (Fig. 5 D–F). In some cases, mitochondria show rudimentary cristae (fragmented) and large, empty central matrix spaces (Fig. 5A, arrows). These changes were similar to those observed in cells dependent on glycolytic metabolism (25), and cristae and matrix swelling are observed in a variety of conditions involving stress and hypoxia (26–28). In addition, the cristae fragmentation in SIV-infected macaques produced a honeycomb-like pattern in cross-section (Fig. 5A, asterisks), reflecting mitochondria under stress conditions. While there were fewer dense granules per mitochondrion in SIV infection compared to healthy controls (Fig. 5G), granule size was significantly larger (Fig. 5 H and I). Mitochondria not containing dense granules were much larger than mitochondria with granules, and a corresponding decrease in the density of their matrices were noted.

After SIV-infected ileal loops were incubated with *L. plantarum*, TEM images revealed a mitochondrial morphology intermediate between healthy controls and SIV-infected ileal loops without bacteria. While the area of the field occupied by mitochondrial mass was still lower, similar to that of SIV⁺ animals (Fig. 5A), the average mitochondrion area was improved (Fig. 5B). Mitochondria morphology was characterized by less circularity compared to both healthy controls and those SIV⁺, with a tubular shape similar

to that of healthy controls. (Fig. 5 D–F). Still evident, some mitochondria had a honeycomb pattern (Fig. 5A, asterisks) with no clear definition of cristae. Although the number of dense body granules did not change from SIV⁺ animals, the granule size was larger, likely indicating increased capacity to accumulate calcium phosphate as a result of improved membrane potential. Our findings identify an accumulation of aberrant mitochondria with lower mass and disrupted distribution and morphology as a result of SIV/HIV enteropathy.

To investigate the role of *L. plantarum* in promoting mitochondrial biogenesis in inflamed gut mucosa during SIV infection, we measured the expression of mitochondrially encoded genes from ileal tissue following *L. plantarum* administration as compared to untreated controls. Mitochondrial genes encoding subunits of complex I (ND1, ND2, ND3, ND4, ND4L, ND5, and ND6), complex III (CTYB), complex IV (COX1, COX2, and COX3), and complex V (ATP6, ATP8) were all down-regulated in SIV infection compared to uninfected controls (Fig. 6A). Administration of *L. plantarum* increased the expression of all these genes, supporting the notion that *L. plantarum* improves the gene expression of key subunits of the electron transport chain in chronic SIV infection. In addition, the decreased expression of genes associated with fatty acid metabolism in SIV infection was reversed after exposure to *L. plantarum*, indicating an improved capacity to utilize fatty acids for energy (Fig. 6B). Increased gene-expression levels of PGC-1α following administration of *L. plantarum* suggested that host mitochondrial metabolism and biogenesis may be a repair mechanism for gut homeostasis. Furthermore, accumulation of dicarboxylic acylcarnitines, a marker of impaired fatty acid β-oxidation in chronic SIV infection, was reduced after administration of *L. plantarum* (Fig. 6C). These findings further elucidate the positive impact of bacteria at improving mitochondrial mass, morphology, and energy-producing pathways.

We assessed functional restoration of mitochondria by metabolomic analysis of luminal contents from intestinal loops with or
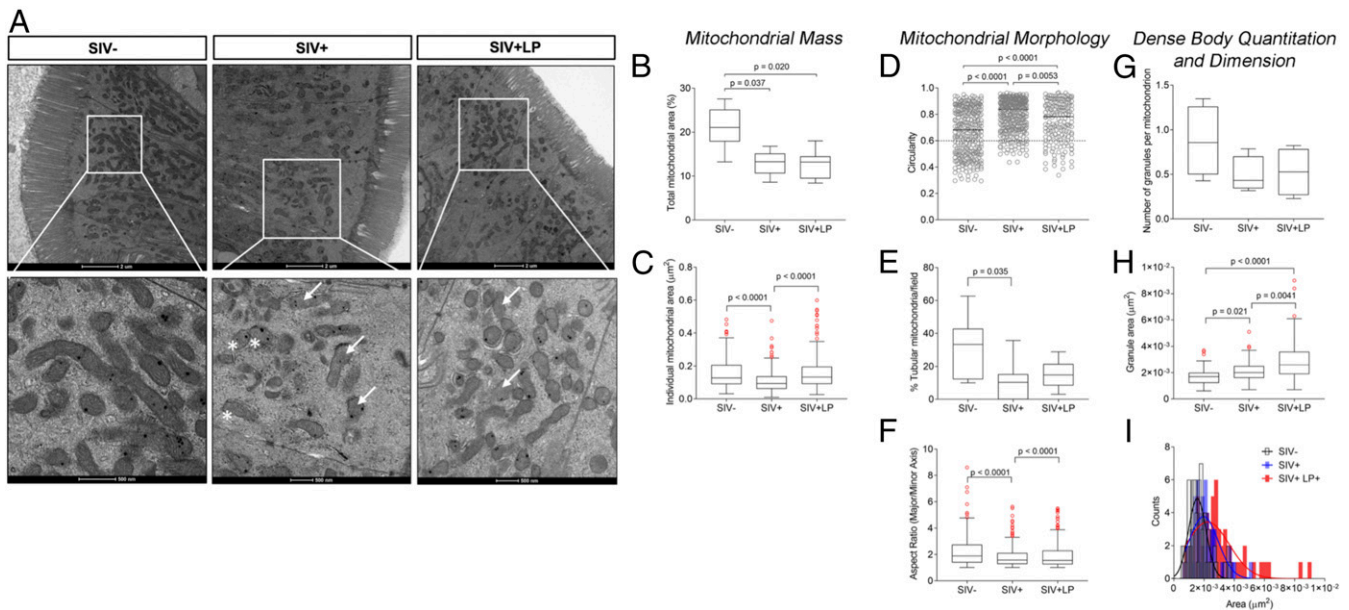
Fig. 5. Protective effects of *L. plantarum* on mitochondrial structure and density in SIV-infected gut. (A) Mitochondrial structure and morphology in apical enterocytes of ileum from healthy controls (n = 4) and SIV-infected macaques (n = 4) with and without *L. plantarum* administration (n =4) (Scale bars, 2 μm; 500 nm in the enlargments.). Mitochondrial mass was evaluated using (B) total mitochondrial area (%) and (C) individual mitochondrial area (μm²). Mitochondrial morphology was assessed using (D) circularity, (E) tubularity, and (F) the collective aspect ratio. Granule bodies and their dimensions were measured by (G) enumeration per mitochondrion, (H) individual granule area (μm²), and (I) collective size per granule count. Data are reported as Tukey's box plots showing median and 1.5IQR. Outliers, shown as empty circles, were included in the statistical analysis.
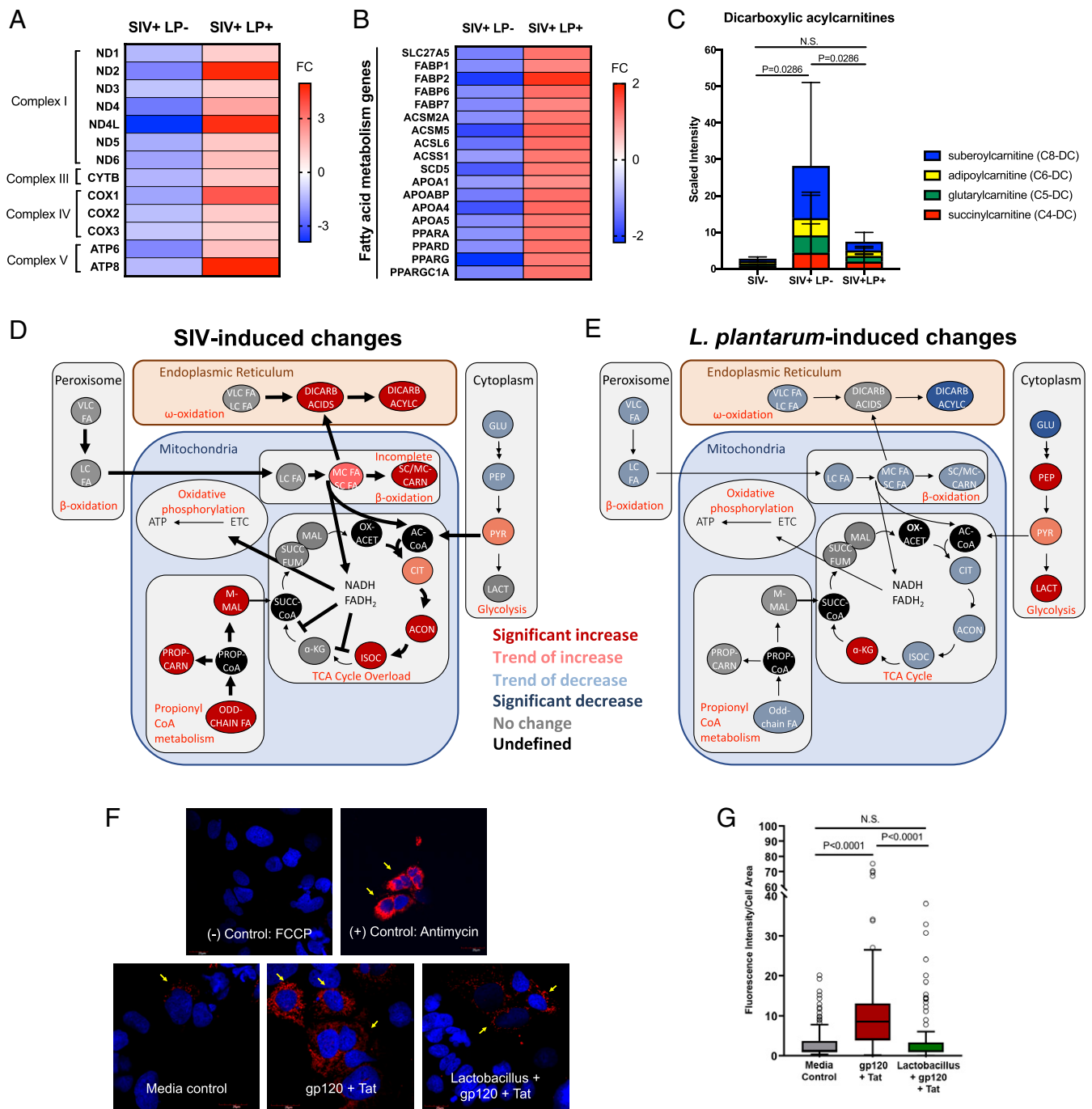
Fig. 6. *L. plantarum* remodels host mitochondrial bioenergetics and ROS production in SIV infection. Heatmap of (*A*) mitochondria-encoded genes and (*B*) genes regulating fatty acid metabolism in the ileum of chronic SIV-infected macaques after incubation with *L. plantarum* for 5 h ($n = 4$ in SIV-LP$^+$ group, $n = 4$ in SIV$^+$ LP$^+$ group). (*C*) Metabolomic analysis of fatty acid components of ileal contents revealed significant changes in the presence of dicarboxylic acylcarnitines ($P < 0.05$). Metabolite intermediates involved in mitochondrial bioenergetics were altered in (*D*) chronic SIV infection and (*E*) after administration of *L. plantarum*. (*F*) Mitochondrial ROS production (yellow arrows, 40×, zoom 2.5×) following treatment with HIV gp120 + Tat and cell-free *L. plantarum* supernatant in Caco-2 cells. (*G*) Data are reported as Tukey's box plot (median and interquartile range), showing MitoSOX fluorescence intensity data normalized by cell area, quantified with ImageJ on at least 100 cells per condition. Statistical analysis was performed with ANOVA followed by Kruskal–Wallis post hoc test for multiple comparisons. Open circles represent outliers, which were included in the statistical analysis. N.S., not significant.

without *L. plantarum* administration. While free fatty acid metabolite levels decreased in SIV infection, short- and medium-chain fatty acids were increased, indicating a lower catabolism of fatty acids that do not use the carnitine transporters (Fig. 6*D*). In support of this notion, fatty acids are diverted to peroxisomal and microsomal fatty acid ω-oxidation to compensate for incomplete mitochondrial

β-oxidation. The impact of SIV infection on mitochondrial function in the gut was characterized by a metabolic switch to induce lipolysis and production of free fatty acids, excessive and incomplete fatty acid β-oxidation, and accumulation of organic acid intermediates of the tricarboxylic acid (TCA cycle) leading to TCA overload. Following *L. plantarum* administration, significant decreases in

ω-oxidation derived products were accompanied by modest decreases in mitochondrial β-oxidation intermediates and members of the TCA cycle (Fig. 6E). Our data suggest that *L. plantarum* promptly alleviates TCA overload by directly utilizing fatty acids or indirectly influencing host metabolic enzymes. There were no significant changes in glycolysis associated with SIV infection. However, a similar level of increased glycolytic flux and lactate production was observed following *L. plantarum* administration in both SIV-infected and uninfected ileal loops, suggesting that *L. plantarum* increased glycolytic intermediates regardless of infection status (*SI Appendix*, Fig. S11). Therefore, glycolysis may not play a major role in SIV pathogenesis in the gut and that luminal contents represent a combination of bacterial-derived as well as host-derived metabolites, as we have previously reported (29). To investigate whether *L. plantarum* impacts mitochondrial ROS production, we measured mitochondrial-derived ROS using MitoSOX staining of Caco-2 epithelial cell cultures (Fig. 6F). Addition of cell-free *L. plantarum* supernatant prevented the increase in mitochondrial ROS production associated with HIV gp120 and Tat treatment (Fig. 6G), suggesting a potential mechanism of repair associated with mitochondrial oxidative phosphorylation.

PPARα-Mediated Metabolic Remodeling and Rapid Repair of Intestinal Epithelial Barrier.

We sought to identify the molecular signaling mechanism of mitochondrial restoration in intestinal loops following *L. plantarum* administration. Analysis of the differential gene expression in SIV-infected animals with *L. plantarum* compared to untreated SIV-infected controls identified PPARα/RXRα signaling to be suppressed in SIV infection but activated after administration of *L. plantarum* (Fig. 7A). Further examination of PPARα target genes showed that *L. plantarum* exposure recovered expression of genes involved in fatty acid metabolism that were down-regulated by SIV infection (Fig. 7B). We cannot, however, exclude a possibility that PPARα activation may also have a direct effect on intestinal barrier gene expression, which has also been implicated in our dataset (*SI Appendix*, Fig. S12).

To validate our findings of *L. plantarum*-driven PPARα activation in vivo, we utilized Caco-2 cell cultures in vitro and examined the effect of the cell-free *L. plantarum* supernatant media on intestinal epithelial cells. The bacterial supernatant induced marked activation of PPARα expression, which was comparable to the magnitude of a PPARα agonist, fenofibrate (Fig. 7C). It is possible that this mechanism involves the up-regulation of pyruvate dehydrogenase kinase 4 (PDK4), a downstream gene of PPARα (along with others) that controls the metabolic switch between aerobic glycolysis and fatty acid metabolism (Fig. 7D). The enhancement of PDK4 after incubation with *L. plantarum* supernatant suggests that the increased fatty acid metabolism was the result of PDK4 up-regulation.

We investigated whether fenofibrate, a known PPARα agonist, may restore mitochondrial function in the context of HIV infection or prevent virus-induced damage. By using the extracellular flux analyzer and oxygen consumption rate (OCR) measurements in Caco-2 cells, we found that pretreatment with fenofibrate for 1 h prevented the moderate decrease in ATP production associated with HIV proteins gp120 and Tat treatments (Fig. 7E). Fenofibrate prevented the decrease in basal respiration (*SI Appendix*, Fig. S13A) and spare respiratory capacity (*SI Appendix*, Fig. S13B), highlighting its potential use to rescue ATP-linked mitochondrial respiration in HIV infection in patients. Other potential candidates for mitochondrial repair, such as the glutathione precursor *N*-acetyl-cysteine, MitoTempo (a mitochondrially targeted scavenger of mitochondrial superoxide anion), and the PPARγ agonist rosiglitazone did not prevent HIV-associated decrease in spare respiratory capacity (*SI Appendix*, Fig. S14). No glycolytic changes were observed on extracellular acidification rate following the addition of gp120, Tat, or fenofibrate (*SI Appendix*,

Fig. S15). To support our findings in Seahorse measurements of OCR, we determined complex I- and complex II-driven mitochondrial ATP synthesis rate by a previously established protocol. While HIV gp120 + Tat treatment significantly decreased OCR in the Seahorse assay, we did not observe changes in complex I- and complex II-driven ATP synthesis, suggesting that the addition of gp120 + Tat may inhibit fatty acid oxidation through complex III–V, which might be the predominant source of energy in the cells (Fig. 7 F and G). Furthermore, the addition of fenofibrate significantly increased OCR in the Seahorse assay while decreasing complex I- and complex II-driven ATP synthesis, suggesting that fatty acid β-oxidation may be enhanced (30) at the expense of complex I- and II-driven glucose oxidation (31), as previously shown. Finally, pretreatment with fenofibrate or *L. plantarum* supernatant prevented disruption of epithelial tight junctions with HIV gp120 and Tat (Fig. 7 H and I). Our data suggest that PPARα activation plays a critical role in protection against HIV-induced intestinal barrier damage through improving mitochondrial function (Fig. 7J).

Discussion

The success of current therapies and future strategies for HIV eradication depends on near-complete recovery of the gut mucosal compartment in HIV-infected patients (32). Even long-term ART has not resulted in complete repair of gut lymphoid tissues consistently in many HIV-infected individuals due to the presence of low levels of residual viral replication and chronic inflammation, and suboptimal regeneration of immune cells (33, 34). ART can effectively suppress viral replication but lacks the ability to repair and renew disrupted lymphoid compartments. Substantial efforts have been made to better incomplete immune recovery. However, it remains underinvestigated why the gut epithelial compartment, which has robust renewal capacity from intestinal stem cells, is not fully renewed structurally and functionally. Using the intestinal loop model in SIV-infected macaques, we investigated enteropathic effects of SIV infection and their reversal by probiotic *L. plantarum* administration. This model allowed us to collect several samples within the same animal to elucidate host–microbe interactions in virally inflamed gut mucosa. Our study identified impaired mitochondrial function and PPARα signaling as a defining mechanism that contributes to gut epithelial barrier disruption in SIV and HIV infection. We demonstrate that intestinal barrier integrity and function can be rapidly restored by probiotic *L. plantarum* through PPARα activation independent of complete mucosal immune recovery.

Our study maps several steps in mitochondrial function that are disrupted during SIV infection. First, mitochondrial morphology in the intestinal epithelial cells exhibit less mitochondrial mass, increased circularity, and fewer dense body granules, suggesting potentially altered mitochondrial sequestration of Ca^{2+}, mitochondrial permeability, and apoptosis. Second, inclusion bodies and cristae loss may represent accumulation of misfolded proteins as a result of increased oxidative stress and failure to assemble subunits of, for example, mitochondrial ATPase (35). Most importantly, disrupted mitochondrial morphology is consistent with functional deficit. Inhibition of fatty acid β-oxidation of short- and medium-chain fatty acids in the gut occurred in both SIV and HIV infection and correlated with structural distribution of ZO-1 tight junction protein. Large numbers of mitochondria observed in apical enterocytes suggest that regulation of cell–cell junctions are linked to mitochondrial ATP production. Using inhibitors of mitochondrial complexes I, III, and V, we show that reducing mitochondrial ATP production leads to disruption of ZO-1 expression. Our data show that metabolic and transcriptional reprogramming of intestinal epithelial cells driving intestinal barrier permeability implicates
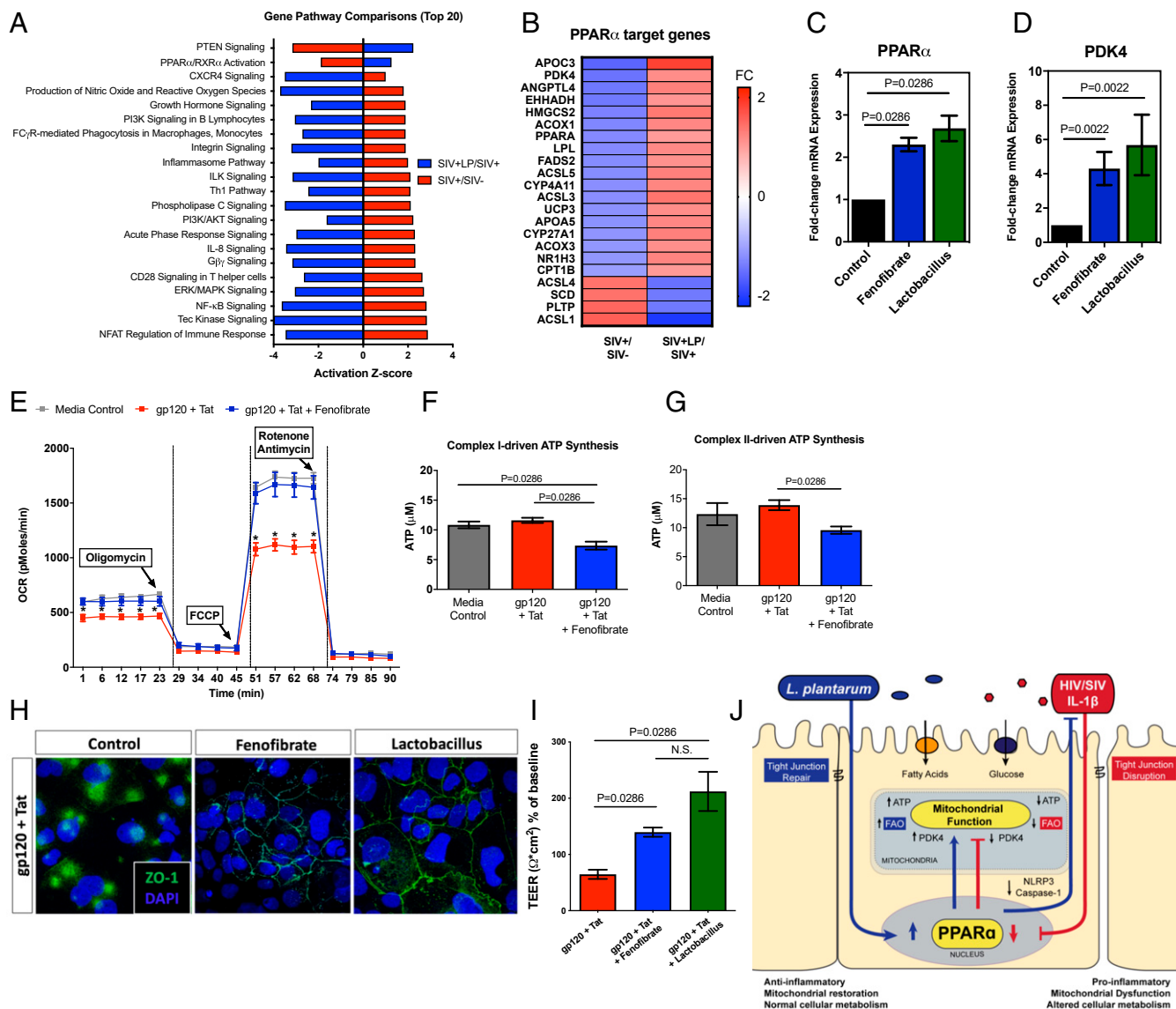
Fig. 7. PPARα-mediated metabolic remodeling restores mitochondrial function and epithelial tight junction integrity. (*A*) Canonical gene pathway analysis of significantly altered genes (−1.5 < FC >1.5, *P* < 0.05) was performed on gene-expression microarrays using Ingenuity Pathway Analysis. (*B*) Heatmap of PPARα target genes during chronic SIV infection and after administration of *L. plantarum*. (*C*) Caco-2 cells treated for 24 h with fenofibrate (10 μM) or *L. plantarum* cell-free supernatant (1:10 dilution in MEM media) were used in measurement of PPARα expression by real-time PCR. (*D*) Expression of PPARα target gene PDK4 was increased compared to control. (*E*) OCR was measured by Seahorse XFe24 after Caco-2 cells were pretreated with fenofibrate (10 μM) or DMSO for 1 h before treatment with HIV gp120 (0.1 μg/mL) + Tat (1.4 μg/mL) for 5 h. Addition of fenofibrate reduced (*F*) complex I- and (*G*) complex II-driven ATP synthesis. Effects of fenofibrate and *L. plantarum* supernatant on epithelial permeability was evaluated using (*H*) immunohistochemical staining of ZO-1 tight junction protein expression (magnification: 63×) and (*I*) TEER measurements. (*J*) An illustration depicting metabolic regulation of gut barriers in SIV infection and repair pathways following administration of *L. plantarum*. N.S., not significant.

mitochondrial dysfunction and this can also increase risk of systemic infection (36).

We previously reported that increased IL-1β expression in Paneth cells drives early disruption of gut barriers in SIV infection (4). We found that increased IL-1β expression persists through chronic SIV infection and asked whether mitochondrial dysfunction contributes to IL-1β–induced intestinal barrier disruption. Addition of IL-1β or the combination of HIV proteins gp120 and Tat induced epithelial barrier disruption in Caco-2 cells, which associated with a decrease in mitochondrial basal and spare respiratory capacity. Defects in neuronal mitochondrial membrane permeability and epithelial tight junction integrity have been observed following treatment with HIV proteins (18, 37). Our study links the disruption of intestinal epithelial

barrier integrity with mitochondrial dysfunction. Understanding the mechanisms by which the epithelial barrier is disrupted in HIV infection enables the development of novel strategies for mucosal restoration.

Commensal gut microbiota regulate integrity of intestinal epithelial barriers. Gut dysbiosis and leaky intestinal barriers in HIV infection may contribute to microbial translocation and chronic immune activation (38). We previously reported that *L. plantarum* can rapidly repair epithelial barrier integrity at 2.5 d post-SIV infection (4), and sought to investigate whether gut barriers could be repaired in chronic viral infection. Administration of *L. plantarum* in intestinal loops led to rapid restoration of intestinal barrier function independent of CD4+ T cell recovery. This rapid rate of recovery (within 5 h) in SIV-inflamed

gut was remarkable. It was previously reported that *L. plantarum* could strengthen intestinal barriers within 6 h in vitro (39) and in 8 h in chicks in vivo (40). Studies are limited that investigate the impact of direct bacterial administration into intestinal loops and subsequent host mucosal response. Introduction of microbes into intestinal lumen can induce rapid host mucosal responses (9, 41). Our analysis of metabolites from gut luminal contents following the administration of *L. plantarum* revealed information about both host-derived and bacterial-derived metabolic products and mechanisms in host–microbe cometabolism. Many of these metabolites are produced by both microbiota and the host. Transcriptomic and metabolomic analyses of gut tissues identified up-regulation of mitochondrial fatty acid metabolism that may be protective in SIV infection. In diet-induced obese mice, probiotic *Lactobacillus* administration reduced fat accumulation and promoted intestinal barrier function (42, 43). We observed that *L. plantarum* also reduced IL-1β–induced inflammation, which may further alleviate cytokine-induced mitochondrial damage. Our findings reveal the synergism between gut microbes and their host as a mechanism to enhance gut repair and healing during HIV infection and ART.

Transcriptional and metabolic data in our study of *L. plantarum*-administered intestinal loops enabled us to test the hypothesis that activation of PPARα may restore fatty acid metabolism and renew intestinal barrier integrity. Previous studies reported that *Lactobacillus* spp. can modulate lipid metabolism and promote antioxidant capacity in mice and aging adults (42, 44). We show that metabolites from *L. plantarum* can induce PPARα signaling in Caco-2 cells to levels similar to cells stimulated by PPARα agonist fenofibrate. Fenofibrate has been explored to improve mitochondrial biogenesis and function in several disease models (45, 46). In our study, fenofibrate attenuated the decline in mitochondrial spare respiratory capacity and epithelial barrier disruption induced by gp120 and Tat. In accordance with findings in HIV-1 Tat-induced diarrhea (47), our data suggest that PPARα signaling may be critical in intestinal repair pathway to reverse mucosal damage in HIV infection. The promotion of mitochondrial fatty acid oxidation following activation of PPARα is likely due to downstream expression of PDK4, a key component in metabolic switching (48). Our findings from intestinal tissues of SIV-infected rhesus macaques and HIV patients in vivo and epithelial cell cultures in vitro reveal that viral infection down-regulates PDK4 expression, which is overcome by activation of PPARα. Activation of PPARα by fenofibrate also restores intestinal epithelial barriers in vitro, suggesting that leveraging cellular metabolism may be useful in mucosal repair and warrant further investigation in the clinical setting. PPARα agonists have been shown to decrease IL-1β expression by deregulating caspase-1 and NLRP3, which is consistent with our observations following *L. plantarum* administration (49). Fenofibrate has been widely used in human patients to treat dyslipidemia and cardiovascular disease with great success and negligible side effects (50). Despite its ability to reduce coronary heart disease and improve lipid profiles in HIV patients, limited data are available on clinical outcomes (51). We demonstrate that mitochondrial fatty acid metabolism in the intestinal epithelium is impaired in SIV-infected rhesus macaques and in HIV-infected patients. Investigating mechanisms underlying metabolic changes highlight new opportunities for fenofibrate and PPARα signaling in gut mucosal health.

Our basic investigation into the mechanism of how epithelial barriers are regulated in chronic SIV infection paved the way to translational findings that may be leveraged for gut mucosal restoration. In the clinical setting, HIV patients on ART, particularly those receiving HIV protease inhibitors, develop insulin resistance reflected as lipodystrophy and altered fatty acid metabolism (52, 53). It is noteworthy that alterations in mitochondrial fatty acid metabolism are not unique to SIV and HIV infections. Cytomegalovirus, dengue virus, and hepatitis C virus utilize host fatty acid metabolism to enhance viral replication (54, 55). A number of inflammatory enteropathies, including inflammatory bowel disease and type 2 diabetes, share common features with HIV infection (56, 57). Investigation across diseases may provide crucial insight on how to repair "leaky gut," chronic inflammation, and mitochondrial dysfunction. Although more widely used in treatment of lipodystrophy in diabetes patients, fibrate drugs have also been successfully used concurrently with ART treatment to reduce hyperlipidemia in HIV infection (53, 58). Our findings identify additional benefits from the use of fenofibrate for modulating the gut epithelial cell metabolism and functionality. We show that impaired PPARα signaling, mitochondrial mass and morphology, and mitochondrial fatty acid β-oxidation are defining mechanisms for restoring the integrity of gut barriers during chronic SIV infection. Our data highlight the opportunity to elucidate the evolutionary synergism between host mitochondria and gut microbes to restore mucosal health and achieve full immune recovery.

Methods

Animal Experiments and Viral Infection. The study design is described in detail in *SI Appendix*. A total of 16 male rhesus macaques were enrolled in the study, 12 of which were infected intravenous with 1,000 TCID50 of SIVmac251 for 10 wk (chronic infection) and 4 of which served as SIV⁻ controls. Of the 12 SIV-infected macaques, 5 received ART, starting at 10-wk postinfection for at least 10 to 20 wk, while 3 remained untreated (7). At 10-wk postinfection, the remaining 4 SIV-infected macaques, along with 4 uninfected macaques, underwent ligated ileal loop surgery to assess the effects following *L. plantarum* administration. Details of the procedures, sample collection, and data analyses are described in *SI Appendix*. Viral loads, CD4 and CD8 T cell numbers in peripheral blood were determined during the course of infection, as previously reported (7). Statistical analysis is described in *SI Appendix*.

Ethics Statement. All macaques involved in the study were housed at the California National Primate Research Center (CNPRC). The CNPRC is fully accredited by the American Association for Accreditation of Laboratory Animal Care for nonhuman primate housing, breeding, and research. In addition, the CNPRC upholds standards set by the US Department of Agriculture, the Animal Welfare Act, and the Food and Drug Administration. In the duration of the study, animals were observed daily by trained CNPRC animal technicians, and significant health observations recorded. Signs, which are monitored daily, include hydration, stool quality, appetite, attitude, and activity level. Animals were euthanized in accordance with the *AVMA Guidelines for the Euthanasia of Animals: 2013 Edition* (ref. 59, section 2.3).

Human Patient Samples. To translate our findings in HIV, gene-expression data from 15 patients from our previous studies were utilized to investigate fatty acid metabolic genes (2, 60). Written informed consent was obtained from all participants and subsequently approved from the Institution Review Board of the University of California Davis and the protocol is current. Jejunal biopsies were collected from 3 patients in primary HIV infection, after the initiation of ART, and ~1 y after ART interruption. Jejunal biopsies from 2 other ART-naïve patients were taken and compared to 10 HIV-seronegative individuals.

Data Availability. The sequences and metadata reported here are available at the Gene Expression Omnibus (GEO) database (accession no. GSE139271) and National Center for Biotechnology Information (NCBI) Bioproject (accession no. PRJNA578916).

1. S. G. Deeks, S. R. Lewin, D. V. Havlir, The end of AIDS: HIV infection as a chronic disease. *Lancet* **382**, 1525–1533 (2013).
2. S. Sankaran *et al.*, Rapid onset of intestinal epithelial barrier dysfunction in primary human immunodeficiency virus infection is driven by an imbalance between immune response and mucosal repair and regeneration. *J. Virol.* **82**, 538–545 (2008).
3. C. Heise, C. J. Miller, A. Lackner, S. Dandekar, Primary acute simian immunodeficiency virus infection of intestinal lymphoid tissue is associated with gastrointestinal dysfunction. *J. Infect. Dis.* **169**, 1116–1120 (1994).
4. L. A. Hirao *et al.*, Early mucosal sensing of SIV infection by paneth cells induces IL-1β production and initiates gut epithelial disruption. *PLoS Pathog.* **10**, e1004311 (2014).
5. M. Guadalupe *et al.*, Viral suppression and immune restoration in the gastrointestinal mucosa of human immunodeficiency virus type 1-infected patients initiating therapy during primary or chronic infection. *J. Virol.* **80**, 8236–8247 (2006).
6. G. Marchetti *et al.*, Microbial translocation is associated with sustained failure in CD4+ T-cell reconstitution in HIV-infected patients on long-term highly active antiretroviral therapy. *AIDS* **22**, 2035–2038 (2008).
7. D. Verhoeven, S. Sankaran, M. Silvey, S. Dandekar, Antiviral therapy during primary simian immunodeficiency virus infection fails to prevent acute loss of CD4+ T cells in gut mucosa but enhances their rapid restoration through central memory T cells. *J. Virol.* **82**, 4016–4027 (2008).
8. O. Kis *et al.*, HIV-1 alters intestinal expression of drug transporters and metabolic enzymes: Implications for antiretroviral drug disposition. *Antimicrob. Agents Chemother.* **60**, 2771–2781 (2016).
9. M. Raffatellu *et al.*, Simian immunodeficiency virus-induced mucosal interleukin-17 deficiency promotes Salmonella dissemination from the gut. *Nat. Med.* **14**, 421–428 (2008).
10. D. M. Dinh *et al.*, Intestinal microbiota, microbial translocation, and systemic inflammation in chronic HIV infection. *J. Infect. Dis.* **211**, 19–27 (2015).
11. J. D. Estes *et al.*, Damaged intestinal epithelial integrity linked to microbial translocation in pathogenic simian immunodeficiency virus infections. *PLoS Pathog.* **6**, e1001052 (2010).
12. E. Rath, A. Moschetta, D. Haller, Mitochondrial function—Gatekeeper of intestinal epithelial cell homeostasis. *Nat. Rev. Gastroenterol. Hepatol.* **15**, 497–516 (2018).
13. A. Wang *et al.*, Targeting mitochondria-derived reactive oxygen species to reduce epithelial barrier dysfunction and colitis. *Am. J. Pathol.* **184**, 2516–2527 (2014).
14. S. A. Younes *et al.*, Cycling CD4+ T cells in HIV-infected immune nonresponders have mitochondrial dysfunction. *J. Clin. Invest.* **128**, 5083–5094 (2018).
15. K. Brinkman, J. A. Smeitink, J. A. Romijn, P. Reiss, Mitochondrial toxicity induced by nucleoside-analogue reverse-transcriptase inhibitors is a key factor in the pathogenesis of antiretroviral-therapy-related lipodystrophy. *Lancet* **354**, 1112–1115 (1999).
16. E. Cassol *et al.*, Plasma metabolomics identifies lipid abnormalities linked to markers of inflammation, microbial translocation, and hepatic function in HIV patients receiving protease inhibitors. *BMC Infect. Dis.* **13**, 203 (2013).
17. T. Roumier *et al.*, Mitochondrion-dependent caspase activation by the HIV-1 envelope. *Biochem. Pharmacol.* **66**, 1321–1329 (2003).
18. H. Lecoeur *et al.*, HIV-1 Tat protein directly induces mitochondrial membrane permeabilization and inactivates cytochrome c oxidase. *Cell Death Dis.* **3**, e282 (2012).
19. I. I. Ivanov, K. Honda, Intestinal commensal microbes as immune modulators. *Cell Host Microbe* **12**, 496–508 (2012).
20. C. A. Lozupone *et al.*, Alterations in the gut microbiota associated with HIV-1 infection. *Cell Host Microbe* **14**, 329–339 (2013).
21. I. Vujkovic-Cvijin *et al.*, Dysbiosis of the gut microbiota is associated with HIV disease progression and tryptophan catabolism. *Sci. Transl. Med.* **5**, 193ra91 (2013).
22. T. W. Glavan *et al.*, Gut immune dysfunction through impaired innate pattern recognition receptor expression and gut microbiota dysbiosis in chronic SIV infection. *Mucosal Immunol.* **9**, 677–688 (2016).
23. G. d'Ettorre *et al.*, Probiotic supplementation promotes a reduction in T-cell activation, an increase in Th17 frequencies, and a recovery of intestinal epithelium integrity and mitochondrial morphology in ART-treated HIV-1-positive patients. *Immun. Inflamm. Dis.* **5**, 244–260 (2017).
24. O. Miró *et al.*, Mitochondrial effects of HIV infection on the peripheral blood mononuclear cells of HIV-infected patients who were never treated with antiretrovirals. *Clin. Infect. Dis.* **39**, 710–716 (2004).
25. J. Van Blerkom, "Developmental failure in human reproduction associated with preovulatory oogenesis and preimplantation embryogenesis" in *Ultrastructure of Human Gametogenesis and Early Embryogenesis*, J. Van Blerkom, P. M. Motta, Eds. (Springer US, Boston, MA, 1989), pp. 125–180.
26. M. Darshi *et al.*, ChChd3, an inner mitochondrial membrane protein, is essential for maintaining crista integrity and mitochondrial function. *J. Biol. Chem.* **286**, 2918–2932 (2011).
27. G. Cenacchi, V. Papa, M. Fanin, E. Pegoraro, C. Angelini, Comparison of muscle ultrastructure in myasthenia gravis with anti-MuSK and anti-AChR antibodies. *J. Neurol.* **258**, 746–752 (2011).
28. M. Damiano *et al.*, Neural mitochondrial Ca2+ capacity impairment precedes the onset of motor symptoms in G93A Cu/Zn-superoxide dismutase mutant mice. *J. Neurochem.* **96**, 1349–1361 (2006).
29. B. L. Golomb, L. A. Hirao, S. Dandekar, M. L. Marco, Gene expression of Lactobacillus plantarum and the commensal microbiota in the ileum of healthy and early SIV-infected rhesus macaques. *Sci. Rep.* **6**, 24723 (2016).
30. S. Jeong, M. Yoon, Fenofibrate inhibits adipocyte hypertrophy and insulin resistance by activating adipose PPARalpha in high fat diet-induced obese mice. *Exp. Mol. Med.* **41**, 397–405 (2009).
31. B. Brunmair *et al.*, Fenofibrate impairs rat mitochondrial function by inhibition of respiratory complex I. *J. Pharmacol. Exp. Ther.* **311**, 109–114 (2004).
32. S. G. Deeks *et al.*; International AIDS Society Scientific Working Group on HIV Cure, Towards an HIV cure: A global scientific strategy. *Nat. Rev. Immunol.* **12**, 607–614 (2012).
33. T. W. Chun *et al.*, Persistence of HIV in gut-associated lymphoid tissue despite long-term antiretroviral therapy. *J. Infect. Dis.* **197**, 714–720 (2008).
34. M. Guadalupe *et al.*, Severe CD4+ T-cell depletion in gut lymphoid tissue during primary human immunodeficiency virus type 1 infection and substantial delay in restoration following highly active antiretroviral therapy. *J. Virol.* **77**, 11708–11717 (2003).
35. L. Lefebvre-Legendre *et al.*, Failure to assemble the alpha 3 beta 3 subcomplex of the ATP synthase leads to accumulation of the alpha and beta subunits within inclusion bodies and the loss of mitochondrial cristae in Saccharomyces cerevisiae. *J. Biol. Chem.* **280**, 18386–18392 (2005).
36. C. A. Thaiss *et al.*, Hyperglycemia drives intestinal barrier dysfunction and risk for enteric infection. *Science* **359**, 1376–1383 (2018).
37. V. Avdoshina *et al.*, The HIV protein gp120 alters mitochondrial dynamics in neurons. *Neurotox. Res.* **29**, 583–593 (2016).
38. J. F. Vázquez-Castellanos *et al.*, Altered metabolism of gut microbiota contributes to chronic immune activation in HIV-infected individuals. *Mucosal Immunol.* **8**, 760–772 (2015).
39. J. Wang *et al.*, Probiotic Lactobacillus plantarum promotes intestinal barrier function by strengthening the epithelium and modulating gut microbiota. *Front. Microbiol.* **9**, 1953 (2018).
40. L. Wang *et al.*, Lactobacillus plantarum restores intestinal permeability disrupted by Salmonella infection in newly-hatched chicks. *Sci. Rep.* **8**, 2229 (2018).
41. J. A. Caserta *et al.*, Development and application of a mouse intestinal loop model to study the in vivo action of Clostridium perfringens enterotoxin. *Infect. Immun.* **79**, 3020–3027 (2011).
42. D. H. Kim *et al.*, Dual function of Lactobacillus kefiri DH5 in preventing high-fat-diet-induced obesity: Direct reduction of cholesterol and upregulation of PPAR-α in adipose tissue. *Mol. Nutr. Food Res.* **61**, 1700252 (2017).
43. R. C. Anderson, A. L. Cookson, W. C. McNabb, W. J. Kelly, N. C. Roy, Lactobacillus plantarum DSM 2648 is a potential probiotic that enhances intestinal barrier function. *FEMS Microbiol. Lett.* **309**, 184–192 (2010).
44. M. S. Lustgarten, L. L. Price, A. Chalé, R. A. Fielding, Metabolites related to gut bacterial metabolism, peroxisome proliferator-activated receptor-alpha activation, and insulin sensitivity are associated with physical function in functionally-limited older adults. *Aging Cell* **13**, 918–925 (2014).
45. J. N. Lee *et al.*, Fenofibrate, a peroxisome proliferator-activated receptor α ligand, prevents abnormal liver function induced by a fasting-refeeding process. *Biochem. Biophys. Res. Commun.* **442**, 22–27 (2013).
46. Y. J. Koh *et al.*, Activation of PPAR gamma induces profound multilocularization of adipocytes in adult mouse white adipose tissues. *Exp. Mol. Med.* **41**, 880–895 (2009).
47. G. Sarnelli *et al.*, HIV-1 Tat-induced diarrhea is improved by the PPARalpha agonist, palmitoylethanolamide, by suppressing the activation of enteric glia. *J. Neuroinflammation* **15**, 94 (2018).
48. Z. Gerhart-Hines *et al.*, Metabolic control of muscle mitochondrial function and fatty acid oxidation through SIRT1/PGC-1α. *EMBO J.* **26**, 1913–1923 (2007).
49. Y. Deng *et al.*, PPARalpha agonist stimulated angiogenesis by improving endothelial precursor cell function via a NLRP3 inflammasome pathway. *Cell. Physiol. Biochem.* **42**, 2255–2266 (2017).
50. R. Scott *et al.*; Fenofibrate Intervention and Event Lowering in Diabetes (FIELD) Study Investigators, Effects of fenofibrate treatment on cardiovascular disease risk in 9,795 individuals with type 2 diabetes and various components of the metabolic syndrome: The Fenofibrate Intervention and Event Lowering in Diabetes (FIELD) study. *Diabetes Care* **32**, 493–498 (2009).
51. D. Samineni, C. J. Fichtenbaum, Fenofibrate in the treatment of dyslipidemia associated with HIV infection. *Expert Opin. Drug Metab. Toxicol.* **6**, 995–1004 (2010).
52. G. Behrens *et al.*, Impaired glucose tolerance, beta cell function and lipid metabolism in HIV patients under treatment with protease inhibitors. *AIDS* **13**, F63–F70 (1999).
53. J. C. Thomas *et al.*, Use of fenofibrate in the management of protease inhibitor-associated lipid abnormalities. *Pharmacotherapy* **20**, 727–734 (2000).
54. E. L. Sanchez, M. Lagunoff, Viral activation of cellular metabolism. *Virology* **479-480**, 609–618 (2015).
55. N. S. Heaton, G. Randall, Dengue virus-induced autophagy regulates lipid metabolism. *Cell Host Microbe* **8**, 422–432 (2010).
56. A. Lonardo *et al.*, Fatty liver is associated with an increased risk of diabetes and cardiovascular disease—Evidence from three different disease models: NAFLD, HCV and HIV. *World J. Gastroenterol.* **22**, 9674–9693 (2016).
57. E. A. Novak, K. P. Mollen, Mitochondrial dysfunction in inflammatory bowel disease. *Front. Cell Dev. Biol.* **3**, 62 (2015).
58. J. G. Gerber *et al.*, Fish oil and fenofibrate for the treatment of hypertriglyceridemia in HIV-infected subjects on antiretroviral therapy: Results of ACTG A5186. *J. Acquir. Immune Defic. Syndr.* **47**, 459–466 (2008).
59. American Veterinary Medical Association, *AVMA Guidelines for the Euthanasia of Animals: 2013 Edition* (American Veterinary Medical Association, Schaumburg, IL, 2013).
60. P. Lerner *et al.*, The gut mucosal viral reservoir in HIV-infected patients is not the major source of rebound plasma viremia following interruption of highly active antiretroviral therapy. *J. Virol.* **85**, 4772–4782 (2011).

MICROBIOLOGY